

# Deaggregation of lifeline risk: Insights for choosing deterministic scenario earthquakes

Nirmal Jayaram<sup>1</sup> and Jack W. Baker<sup>1</sup>

<sup>1</sup>Civil and Environmental Engineering, Stanford University; email: nirmalj@stanford.edu

## ABSTRACT

Probabilistic seismic risk assessment for lifelines is less straightforward than for individual structures. Analytical risk assessment techniques such as the “PEER framework” are insufficient for a probabilistic study of lifeline performance, due in large part to difficulties in describing ground-motion hazard over a region. As a result, Monte Carlo simulation and its variants appear to be the best approach for characterizing ground motions for lifelines. A challenge with Monte Carlo simulation is its large computational expense, and in situations where computing lifeline losses is extremely computationally demanding, assessments may consider only a single “interesting” ground-motion scenario and a single associated map of resulting ground motion intensities.

In this paper, a probabilistic simulation-based risk assessment procedure is coupled with a deaggregation calculation to identify the ground-motion scenarios most likely to produce exceedance of a given loss threshold. The deaggregation calculations show that this “most-likely scenario” depends on the loss level of interest, and is influenced by factors such as the seismicity of the region, the location of the lifeline with respect to the faults and the current performance state of the various components of the lifeline. It is seen that large losses are typically caused by moderately large magnitude events with large average values of inter-event and intra-event residuals, implying that the scenario ground motions should be obtained in a manner that accounts for ground-motion uncertainties. Explicit loss analysis calculations that exclude residuals will demonstrate that the resulting loss estimates are highly biased.

## 1 INTRODUCTION

Probabilistic seismic risk assessment for lifelines is less straightforward than for individual structures. While procedures such as the “PEER framework” have been developed for risk assessment of individual structures, these are not easily applicable to distributed lifeline systems, due in large part to difficulties in describing ground-motion hazard over a region (in contrast to ground-motion hazard at a single site, which is easily quantified using Probabilistic Seismic Hazard Analysis). In the past, researchers have used simplified approaches to tackle the problem of specifying ground motions over a region. In the simplest case, the uncertainties in the ground-motion intensities are ignored, and lifeline risks are studied using the median ground motions predicted by ground-motion models (e.g., Shiraki et al, 2007, Campbell and Seligson, 2004). While this approach reduces the computational burden significantly, ignoring the uncertainties in the ground-motion intensities will result in highly biased risk estimates as shown in this paper subsequently. Sometimes, as a simplification, lifeline risks are assessed using only

those earthquake scenarios that may dominate the ground-motion hazard in the region of interest (e.g., Adachi and Ellingwood, 2008). This approach is helpful practically in reducing computational expense, but suffers from several problems. First, it is difficult to identify the probability of actually incurring the computed losses resulting from a single ground-motion scenario. Second, the scenario earthquake is generally chosen in a somewhat ad hoc manner, and so there is no guarantee that the chosen scenario is the one that is most “interesting” in terms of risk to the lifeline system.

Crowley and Bommer (2006) and more recently Jayaram and Baker (2009a) proposed Monte Carlo simulation (MCS)-based frameworks to forward simulate ground-motion intensities in future earthquakes, which can then be used for the risk assessment of lifelines. The sampling frameworks are based on the form of existing ground-motion models, which is described below. We model ground motion at a site as (e.g., Boore and Atkinson, 2008)

$$\ln(Y_i) = \ln(\bar{Y}_i) + \varepsilon_i + \eta \quad (1)$$

where  $Y_i$  denotes the ground-motion parameter of interest (e.g.,  $S_a(T)$ , the spectral acceleration at period  $T$ ) at site  $i$ ;  $\bar{Y}_i$  denotes the predicted (by the ground-motion model) median ground-motion intensity;  $\varepsilon_i$  denotes the intra-event residual, which is a zero mean random variable with standard deviation  $\sigma_i$ ;  $\eta$  denotes the inter-event residual, which is a random variable with zero mean and standard deviation  $\tau$ . The standard deviations,  $\sigma_i$  and  $\tau$ , are estimated as part of the ground-motion model. The intra-event residual at two sites  $i$  and  $j$  are correlated, and the correlation is a function of the separation distance between the sites. The extent of the correlation can be obtained from spatial correlation models such as that of Jayaram and Baker (2009b) and Wang and Takada (2005).

Crowley & Bommer (2006) describe the MCS approach used to probabilistically sample ground-motion maps. This approach involves simulating earthquakes of different magnitudes on various active faults in the region, followed by simulating the inter-event and the intra-event residuals at the sites of interest for each earthquake. The residuals are then combined with the median ground motions in accordance with Equation 1 in order to obtain the ground motions at all the sites.

In the current work, the simulation approach described above is coupled with a deaggregation calculation that can identify the ground-motion scenario most likely to produce exceedance of a given loss threshold. The results show that the most-likely scenario depends on the loss level of interest, and is influenced by factors such as the seismicity of the region, the location of the lifeline with respect to the faults and the current performance state of the various components of the lifeline. It is also seen that large losses are most likely to be caused by moderately large magnitude earthquakes combined with large positive inter-event and intra-event residuals. The findings illustrate the importance of accounting for ground-motion uncertainty, as

well as provide a basis for a decision maker to choose interesting scenario ground motions for lifeline risk assessment.

## 2 DEAGGREGATION OF SEISMIC LOSS

This section describes the fundamentals of the seismic loss deaggregation procedure which is used in the current study. Deaggregation is the process used to quantify the likelihood that various events could have produced the exceedance of a given loss threshold. For instance, if it is known that the seismic loss exceeds  $x$  units, the likelihood that an event of magnitude  $m$  could have caused the exceedance is given as follows:

$$P(\text{Magnitude} = m | \text{Loss} > x) = \frac{P(\text{Loss} > x, \text{Magnitude} = m)}{P(\text{Loss} > x)} = \frac{\lambda(\text{Loss} > x, \text{Magnitude} = m)}{\lambda(\text{Loss} > x)} \quad (2)$$

where  $\lambda(\text{Loss} > x, \text{Magnitude} = m)$  denotes the recurrence rate of events of magnitude  $m$  causing more than loss  $x$  and  $\lambda(\text{Loss} > x)$  is the recurrence rates of events causing a loss exceedance of  $x$ . These parameters can be estimated using the simulation-based framework described in Section 1.

The likelihoods can also be computed considering multiple parameters such as magnitudes and faults as follows:

$$P(\text{Magnitude} = m, \text{fault} = f | \text{Loss} > x) = \frac{\lambda(\text{Loss} > x, \text{Magnitude} = m, \text{fault} = f)}{\lambda(\text{Loss} > x)} \quad (3)$$

Such calculations are common practice when loss assessments are carried out for a single structure (though most deaggregation calculations estimate the contribution (likelihood) of various earthquake scenarios to ground-motion intensity exceedance rather than loss exceedance). Typical results from the single-site deaggregation computations include the joint likelihoods of magnitudes, rupture distances (distance of the structure from the rupture) and residuals (Equation 1).

In the current work, it is of interest to identify the contributions of magnitudes, rupture locations and residuals (inter-event and intra-event) to lifeline losses. Deaggregation calculations for lifeline losses need to account for the fact that ground motions at multiple sites are of interest. This would mean that a specific distance to the rupture cannot be obtained as is commonly done when a single structure is involved. In the current work, this problem is overcome by specifying the fault on which the rupture lies rather than the distance to any particular site. Further, since each site of interest is associated with a different intra-event residual, deaggregation is used to compute the contribution of the mean intra-event residual (i.e., the average of the intra-event residuals at all sites) rather than the contribution of the intra-event residual at any particular site.

### 3 LOSS ASSESSMENT FOR THE SAN FRANCISCO BAY AREA TRANSPORTATION NETWORK

The deaggregation computations in the current work are based on the loss estimates for an aggregated form of the San Francisco bay area transportation network provided by Jayaram and Baker (2009a). This section describes the details of the aggregated network as well as describes the performance measures considered in the loss assessment process.

Figure 1 shows the deaggregated network along with the various important faults in the San Francisco bay area. The network consists predominantly of freeways and expressways, and has a total of 586 links, 310 nodes and 1,125 bridges. In this network, the traffic originates and culminates in 46 nodes denoted centroidal nodes. Transportation network performance is usually measured in terms of the total travel time of the network (Shiraki et al., 2007 and Stergiou and Kiremidjian, 2006). The total travel time is obtained using the user-equilibrium principle which states that, under equilibrium, each user would choose the path that would minimize his/ her travel time (Bechman et al., 1956). The user-equilibrium formulation is solved by the commonly-used solution technique provided by Frank and Wolfe (1956).

The changes in the network travel time after an earthquake are due to structural damage to bridges which will result in link closures and reduction in the link capacities (The current work considers only the change in the total network travel time, and omits monetary costs due to structural damage.) Thus, the loss assessment is carried out by accounting for the structural damage to bridges caused by each simulated ground-motion map (obtained using the simulation-based procedure described in Section 1) and computing the network travel time in the damaged state (In the current work, only peak-hour demands and travel times are considered.) Figure 2 shows the loss estimates in the form of a recurrence curve, which shows the rate of exceeding various travel times delays. The current work uses these loss estimates (i.e., travel time delays) in the deaggregation calculations.

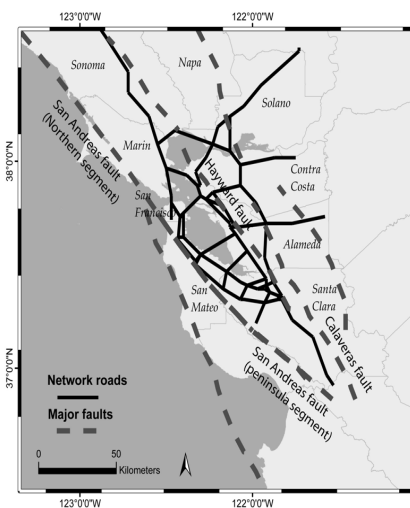
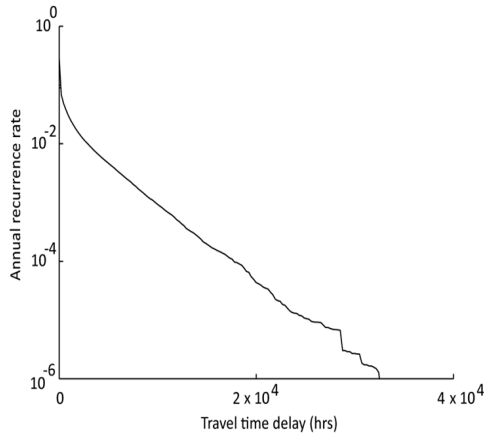


Figure 1. The aggregated San Francisco bay area transportation network.

### 4 RESULTS AND DISCUSSION

This section presents the results from the deaggregation calculations, which include the contribution of magnitudes, faults, inter-event residuals and mean intra-event residuals to lifeline losses. The estimates are obtained using equations similar to 2 and 3, where the required recurrence rates are obtained using the simulation-based loss assessment framework described in the previous sections. For instance, if 100 out of 15,000 simulated events involve an earthquake of magnitude 7 and a loss (i.e., travel time delay) exceeding

10,000 hours,  $P(Loss > 10,000, Magnitude = 7) = 100/15,000$ .



**Figure 2. Recurrence curve for the travel time delay obtained using the simulation-based framework.**

#### 4.1 Contribution of magnitudes and faults to the lifeline losses

Figure 3 shows the contribution (i.e., the likelihood term obtained from Equation 3) of various magnitudes and faults to the probability of exceeding four different travel delay thresholds, namely, 0 hours, 5,000 hours, 10,000 hours and 20,000 hours (The total travel time in the network during normal operating conditions equals 73,000 hours.) In order to obtain the contributions of discrete magnitudes to the loss exceedance, earthquakes of different magnitudes need to be pooled in to bins of select discrete magnitudes. In the current work, the bin size is chosen to be 0.5. For instance, all magnitudes between 7.75 and 8.25 will be

classified as magnitude 8.

Figure 3 shows that, at small loss thresholds, small magnitude events contribute significantly to the loss, which is understandable since small magnitude events are significantly more probable than large magnitude events. Also, as seen from the Figure 3, the loss is typically dominated by events on the northern segment of the San Andreas Fault. This is because the rate of earthquake occurrence on the San Andreas Fault is much larger than that on other faults.

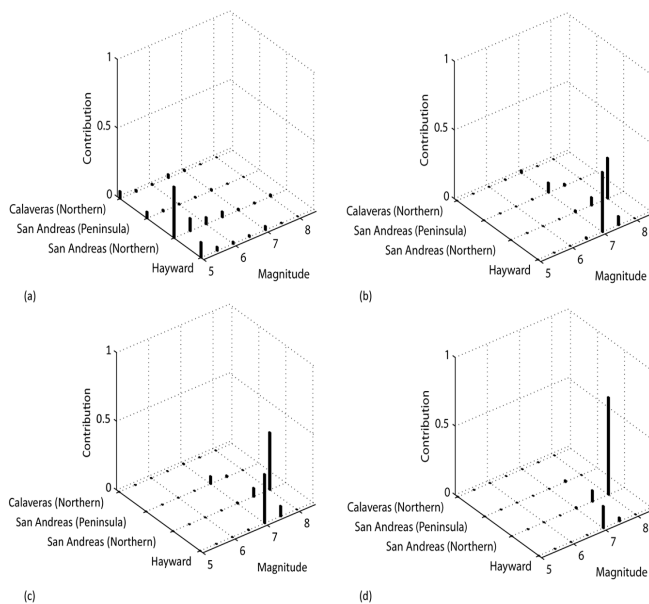


**Figure 3. Joint likelihoods of magnitudes and faults given that travel time delay exceeds (a) 0 hours, (b) 5,000 hours, (c) 10,000 hours and (d) 20,000 hours.**

At moderate loss levels (5,000-10,000 hours), a significant portion of the contribution is shared by earthquake events on the Hayward and the San Andreas Faults. Events of magnitude close to 7 on the Hayward Fault and of magnitude around 8 on the San Andreas Fault are ‘characteristic events’ on the respective faults (USGS, 2003). In other words, these earthquakes are known to occur on a fairly regular basis and hence, are more likely than even some of the smaller magnitude events on these faults. It can be seen from Figure 3 that the characteristic events contribute most to the moderate losses by virtue of the higher likelihoods of occurrence. Further, it is interesting to note that an event of

magnitude 7 on the Hayward has a slightly larger contribution than a much larger event (magnitude 8) on the San Andreas fault. This is due to the fact that the Hayward fault is right down the middle of the network while the San Andreas is on the western end. As a result, an event on the Hayward fault causes moderate damage to all the links in the network, while the San Andreas event causes extensive damage to the west end of the network and very less damage to the east end. The overall effect is a nearly equal contribution to the losses by both the above-mentioned events.

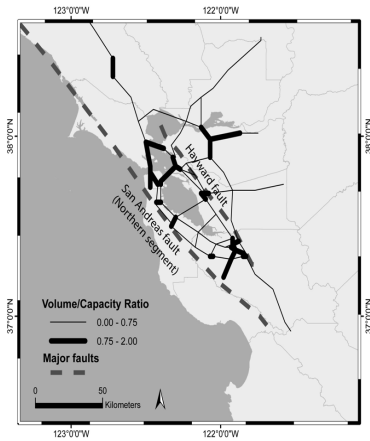


**Figure 4. Level of congestion in the network as indicated by the volume/ capacity ratio.**

At large loss levels (20,000 hours), however, events on the San Andreas Fault again dominate the hazard. Of all the links present in the transportation network, the most congested ones under normal operating conditions are in the western portion of the network. This can be seen from Figure 4 which shows the ratio of the volume of traffic in each link normalized by the link capacity. Large travel time delays are incurred if links that are congested (volume/capacity greater than 0.75) under normal conditions suffer damage increasing the congestion even further. This happens when a moderate to large event occurs on the San Andreas Fault (which is adjacent to several congested links) and has large residuals, and hence such a scenario is the primary cause for large delays in the network.

It can be seen from the above discussion that the most-likely scenario depends on the loss level of interest, and is influenced by factors such as the seismicity of the region, the location of the lifeline with respect to the faults and the performance state of the various components of the

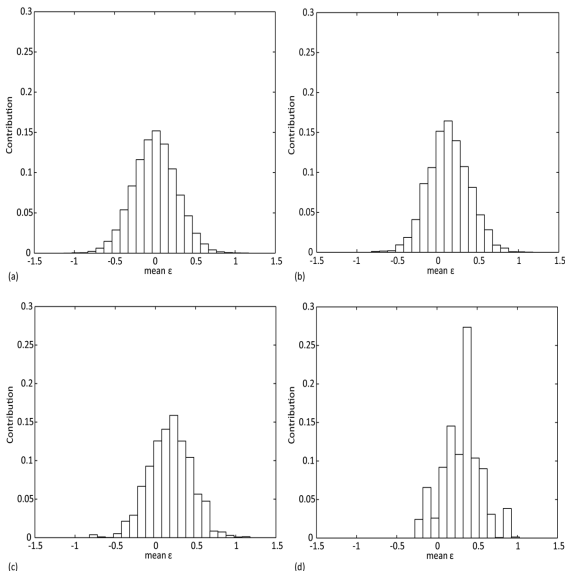


**Figure 5. Joint likelihoods of inter-event residual given that travel time delay exceeds (a) 0 hours, (b) 5,000 hours, (c) 10,000 hours and (d) 20,000 hours.**

lifeline under normal operating conditions. In fact, for certain loss levels, it may not even be possible to choose a single dominating event as shown in Figures 3b and c, which show nearly equal contributions by events on the Hayward and the San Andreas Faults.

#### **4.2 Contribution of inter- and intra-event residuals to the lifeline loss**

Figures 5 and 6 show the contribution of mean intra-event and inter-event residuals to the probability of exceeding four different travel time delay thresholds. As expected, events with residuals close to zero (the mean value) dominate small seismic losses. As the loss level increases, the contribution of large inter-event and large mean

intra-event residuals increases rapidly. It can be seen from Figures 5d and 6d that, at a loss threshold of 20,000 hours, significant contributions are obtained from mean intra-event residuals between 0.3 and 0.5 and inter-event residuals between 1.5 and 3. These results are perhaps not surprising given the large effect that inter-event and intra-event residuals have on the resulting ground motions. Since the inter-event residual is constant across the entire region, a large positive value will increase the ground-motion intensity at every site in the region. As a consequence, appropriate consideration of the inter-event residual is extremely important while assessing lifeline losses than while assessing the losses for a single structure.

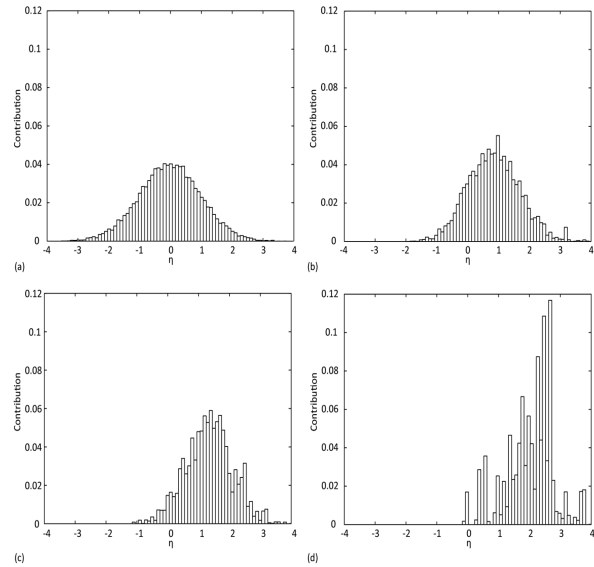


**Figure 6. Joint likelihoods of inter-event residual given that travel time delay exceeds (a) 0 hours, (b) 5,000 hours, (c) 10,000 hours and (d) 20,000 hours.**

Finally, Figures 7 and 8 summarize the findings from the deaggregation calculations, and illustrate the variation in the mean magnitude and the mean residuals of the ground-motion scenarios that contribute to the probability of exceeding various lifeline loss thresholds. For instance, the mean magnitude causing a travel time delay exceeding  $x$  hours is obtained by averaging the magnitudes of all earthquakes that produce a travel time delay greater than  $x$  hours. The figures show that the magnitude, inter-event residual and mean intra-event residual increase

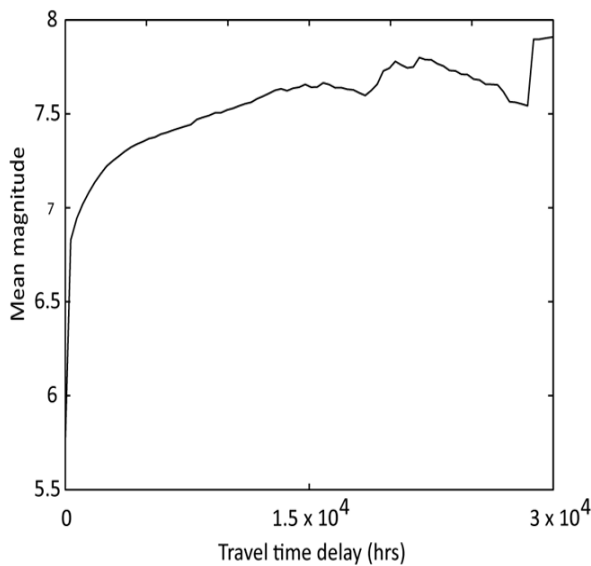


**Figure 7. Mean magnitude of earthquakes producing a travel time delay exceeding a specified threshold.**

rapidly as the travel time delay threshold increases (Some of the wiggles seen at large thresholds are due to small sample sizes at these thresholds.) It is interesting to note that most of the extremely large losses occur at magnitudes well below the maximum (the maximum is 8.05 in this source model), which indicates that large losses are typically caused by moderately large events combined with large values of residuals (Figure 8) as explained previously. This result can be understood intuitively as follows: while “maximum magnitude” events certainly cause large losses, they occur so infrequently that in many cases, more common moderate magnitude events may be more important.

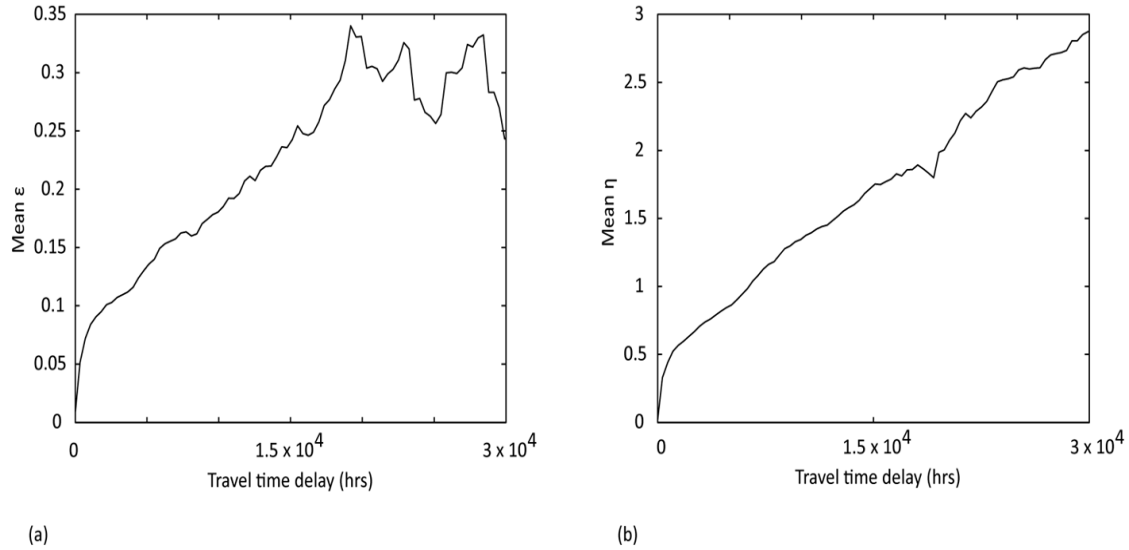


**Figure 8. (a) Average of mean intra-event residual of earthquakes producing a travel time delay exceeding a specified threshold (b) Average of inter-event residual of earthquakes producing a travel time exceeding a specified threshold.**

In order to further emphasize the importance of residuals, in the current work, the loss assessment for the aggregated network was repeated without considering one or both types of residuals (i.e., the inter-event and the intra-event residuals). The recurrence curves obtained are shown in Figure 9. The figure shows that the loss is significantly underestimated if even one of the two types of residuals is not considered. This is to be expected based on the previous observation that the contribution to large loss levels typically comes from events of moderately large magnitude and large positive residuals rather than events of extremely large magnitudes and zero residuals.

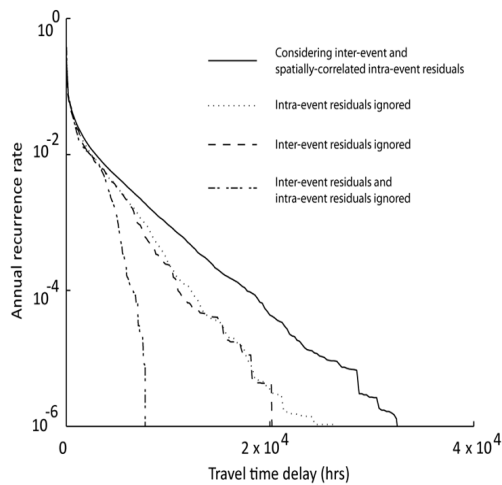


**Figure 9. Recurrence curves obtained without completely accounting for inter-event and intra-event residuals**

### 4.3 Transportation network performance under sample scenario ground-motion maps

This section provides a graphical illustration of why residuals play an important part in determining the losses to the transportation network. The performance of the network is analyzed under three different ground-motion scenarios, namely, A, B and C. All three scenarios result from an earthquake of magnitude 8.1 on the northern segment of the San Andreas Fault, and have a mean intra-event residual of approximately zero. The value of the inter-event residual equals 3.79 in scenario A, -1.64 in scenario B and 0 in scenario C.

Figure 10 graphically shows the performance of

the transportation network under the three ground-motion scenarios. Thicker lines indicate links experiencing larger increases in the travel times. It can be seen that the delays are much greater under scenario A than under scenarios B and C. In fact, the travel time delay in the network equals 32,600 hours under scenario A, 1,550 hours under scenario B and 4,580 hours under scenario C. The significant differences are a result of the differences in the inter-event residual, since the predicted median ground-motion intensities in all these three cases are identical.

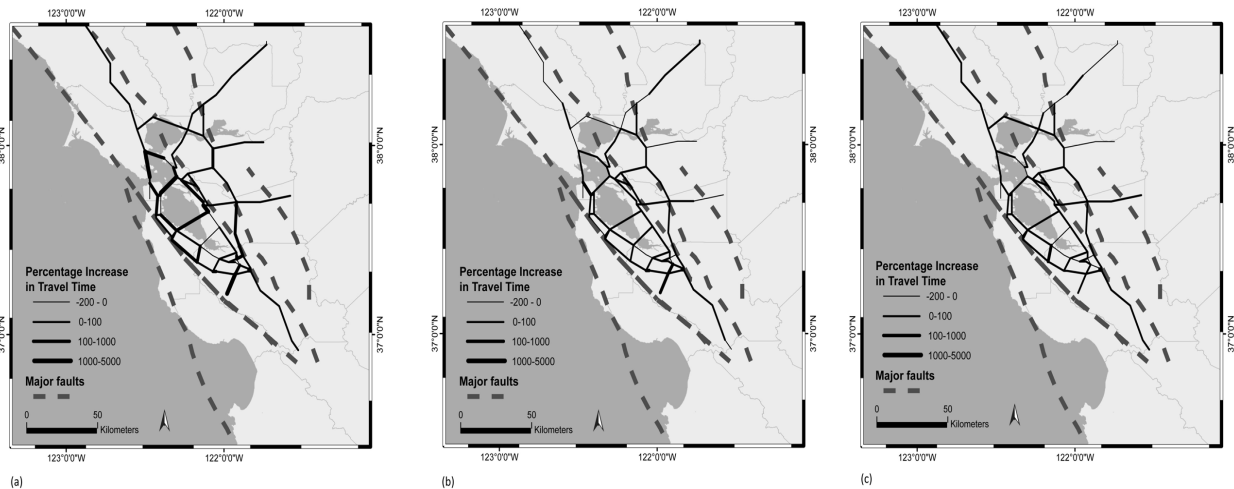


**Figure 10. Performance of the network under three different ground-motion scenarios corresponding to three different inter-event residuals. (a)  $\eta = 3.79$ , (b)  $\eta = -1.64$  and (c)  $\eta = 0$ .**

## 5 CONCLUSIONS

In this paper, a probabilistic simulation-based loss assessment procedure is coupled with a deaggregation calculation that can identify the ground-motion scenarios most likely to produce exceedance of a given loss threshold for a spatially-distributed lifeline system. The deaggregation calculation quantifies the likelihood that various events (magnitudes, faults, inter-event and intra-event residuals) could have produced the exceedance of a given loss threshold. In the current work, deaggregation calculations are performed to identify the likelihoods of earthquake events that cause various levels of travel time delays (the lifeline loss measure) in an aggregated form of the San Francisco bay area transportation network. The deaggregation calculations indicate that the “most-likely” scenario depends on the loss level of interest, and is influenced by factors such as the seismicity of the region, the location of the lifeline with respect to the faults and the performance state of the various components of the lifeline under normal operating conditions. In fact, for certain loss levels, it is seen that two different events (different magnitudes and faults) could have similar contributions to the loss exceedance making it impossible to identify a single most-likely scenario earthquake. The deaggregation calculations also show that large losses are typically caused by moderately large magnitude events with large values of inter-event and intra-event residuals, indicating that it is very important to appropriately account for the residuals in the loss assessment framework. Loss assessments

carried out without accounting for either the inter-event or the intra-event residuals produce highly biased and incorrect loss estimates.

## REFERENCES

Adachi, T., and Ellingwood, B. R. (2008). "Serviceability of earthquake-damaged water systems: Effects of electrical power availability and power backup systems on system vulnerability." *Reliability Engineering and System Safety*, 93,78-88.

Beckman, M. J., McGuire, C. B., and Winsten, C. B. (1956). "Studies in the economics of transportation." *Technical report*, Cowles commission monograph, New Haven, Conn.: Yale University press.

Boore, D. M., & Atkinson, G. M. (2008). "Ground-motion prediction equations for the average horizontal component of PGA, PGV and 5% damped SA at spectral periods between 0.01s and 10.0s." *Earthquake Spectra*, 24(1), 99–138.

Campbell, K. W., and Seligson, H. A. (2004). "Quantitative method for developing hazard-consistent earthquake scenarios." *In Proceeding, 6th U.S. conference and workshop on lifeline earthquake engineering*.

Crowley, H., and Bommer, J. J. (2006). "Modelling seismic hazard in earthquake loss models with spatially distributed exposure." *Bulletin of Earthquake Engineering*, 4(3), 249–273.

Frank, M., and Wolfe, P. (1956). "An algorithm for quadratic programming." *Naval Research Logistics Quarterly*, 3, 95–110.

Jayaram, N., and Baker, J. W. (2009a). "Efficient sampling techniques for seismic risk assessment of lifelines." *The 10th International Conference on Structural Reliability and Safety* (accepted for publication).

Jayaram, N., and Baker, J. W. (2009b). "Correlation model for spatially-distributed ground-motion intensities." *Earthquake Engineering and Structural Dynamics* (accepted for publication).

Stergiou, E., and Kiremidjian, A. S. (2006). "Treatment of uncertainties in seismic risk analysis of transportation systems." *Technical report No. 154*, Blume earthquake engineering center, Stanford University.

Shiraki, N., Shinozuka, M., Moore II, J. E., Chang, S. E., Kameda, H., and Tanaka, S. (2007). "System risk curves: Probabilistic performance scenarios for highway networks subject to earthquake damage." *Journal of Infrastructure Systems*, 213(1), 43–54.

Wang, M. and Takada, T. (2005). "Macrosatial correlation model of seismic ground motions." *Earthquake Spectra* 21(4), 1137-1156.